

ARTICLE

A Diagnostic Method for Fog Forecasting Using Numerical Weather Prediction (NWP) Model Outputs

Aditi Singh*  R.S. Maheskumar Gopal R. Iyengar

Ministry of Earth Sciences, Lodi Road, New Delhi, 110003, India

ARTICLE INFO

Article history

Received: 16 September 2022

Revised: 12 October 2022

Accepted: 13 October 2022

Published Online: 19 October 2022

Keywords:

Fog

Diagnostic method

Northern plains

Winter

Threshold

ABSTRACT

An attempt has been made in the present study to forecast fog with a diagnostic method using the outputs of global NWP model. The diagnostic method is based on the combination of thresholds of meteorological variables involved in fog formation. The thresholds are computed using the observations during fog. These thresholds are applied to the output of a global NWP model for forecasting fog. The occurrence of fog is a common phenomenon during winter season over the northern plains of India. The diagnostic method is used to predict fog occurrences over three stations in north India. The proposed method is able to predict both occurrences and non-occurrences of fog at all the three stations. It is found that 94% of the fog events forecasted by the model using the diagnostic method have been actually observed at the selected stations. The performance of method in predicting fog is found best over Delhi with the highest accuracy (0.61) and probability of detection (0.60). The study signifies that diagnostic approach based on the output of a global model is a useful tool for predicting fog over a single location.

1. Introduction

Fog formation over any region causes low visibility conditions leading to hazardous conditions worldwide and disrupting the normal life and all the modes of transport such as road, rail, air and marine traffic^[1-5]. The aviation sector suffers economic losses in different parts of the world due to fog^[6-10]. Thus, several climatological studies and field campaigns have been conducted focusing on some of the busiest airports around the world^[11-14]. In

addition, numerous field and numerical studies have been conducted worldwide^[15-21,23-27] to understand the formation and development of fog. The studies indicated that a number of factors such as near surface radiative cooling profiles, topography, land surface characteristics, pollution, boundary layer temperature, humidity, wind speed and wind direction are responsible for fog formation over any surface. The understanding of local weather conditions that lead to fog, plays a major role in the operational forecasting of fog. Fog is a suspension of water droplets in the

*Corresponding Author:

Aditi Singh,

Ministry of Earth Sciences, Lodi Road, New Delhi, 110003, India;

Email: aditi.singh76@gov.in

DOI: <https://doi.org/10.30564/jasr.v5i4.5068>

Copyright © 2022 by the author(s). Published by Bilingual Publishing Co. This is an open access article under the Creative Commons Attribution-NonCommercial 4.0 International (CC BY-NC 4.0) License. (<https://creativecommons.org/licenses/by-nc/4.0/>).

atmosphere near the surface which are formed due to low temperature, high relative humidity and stable conditions. The water droplets condense on aerosols under polluted conditions. The prevalence of stable atmospheric conditions over the northern plains of India during winter season aids in formation of fog. The northern plains of India frequently experience western disturbances (WDs), low pressure systems observed in midlatitude westerlies which move from west to east in all seasons but are most prominent over Himalayas during the months of December to March. In winter season WDs provide sufficient moisture and stable conditions required for formation of fog over the northern plains of India [28,29]. The plains of north India are invariably affected by fog every year between the end of December to beginning of January due to typical prevailing meteorological and terrain conditions [30,31]. The studies conducted over India suggest an increase in fog events over the Indo-Gangetic basin (IGB) encompassing northern plains of India during the last decade [32,33] in the winter months. The airports, road and rail networks located in this region of India are affected by fog in winter months of December and January. According to a study [34], Indira Gandhi International Airport (IGIA) in Delhi suffered a total economic loss of approximately \$3.9 million during 2011-2016 due to fog. Thus, the prediction of fog over the northern plains of India is significant for safe and efficient operations of all the modes of travel/transport. However, the accurate prediction of fog has long been a challenge for both the operational forecasters and the present numerical weather prediction (NWP) models. The present NWP models are not able to predict the fog due to lack of appropriate fog physics. The cloud schemes used in the operational NWP models are designed to represent the high-level clouds and precipitation and not the ground level fog. Also, the processes such as gravitational settling on the ground and surface layer turbulence involved in formation of fog are not included in the cloud scheme. Another reason is the coarse resolution of NWP models. The local weather conditions are not well represented in the coarse grid models and thus these models fail to accurately predict fog which is a local phenomenon. The third reason is that operational fog forecasting is based upon the model post processor and is not directly obtained from the model. The evolution of fog is a complex process and is related to turbulence [35] and the impact of turbulence cannot be represented in model post processor. Thus, a fog diagnostic method based on the model post processor output has been developed for fog prediction. One of the diagnostic methods used to predict fog with model post processor output is visibility diagnosis method. According to World Meteorological Organization (WMO), fog

is a surface weather condition and occurs when surface visibility is less than 1000 meters (m). Thus, the visibility one of the variables diagnosed from the model postprocessor output is used to predict fog. Most of the operational model uses the Kunkel [36] fog visibility formulation based on surface liquid water content (LWC) to determine the visibility during fog. The verification studies conducted over different parts of world such as East China, North America and India [37-39] indicate a low performance of visibility diagnosis method. The multi-rule fog diagnosis method [40,37,41] was developed as the visibility diagnosis method exhibit poor performance in predicting fog. The study conducted by Zhou and Du [37] used the liquid water content (LWC), cloud base/top rule and surface relative humidity (RH)-wind rule. The study concluded that RH-wind rule with $2 \text{ m RH} > 90\%-95\%$ and wind speed at $10 \text{ m} < 2 \text{ m}\cdot\text{s}^{-1}$ works better when both the parameters are considered together than any of the parameters LWC or cloud base/top on individual basis. Another study by Payra and Mohan [41] mentioned that cloud base/top rule is good for coastal or marine fog and not for shallow or ground fog and utilized the two-level approach using RH-wind rule along with temperature gradient rule. Radiation and advection, two types of fog are generally observed in India. The advection fog occurs in the forward sector whereas the radiation fog occurs in the rear sector of a western disturbance. Radiation fog occurs due to radiative cooling of earth's surface during nighttime with favorable meteorological conditions of low wind speed, high relative humidity, clear sky and stable conditions.

The present study focuses on the prediction of radiation fog over the northern plains of India using the diagnostic method based on the threshold values of relative humidity at 2 m, dew point depression at 2 m and wind speed at 10 m. The threshold values of the variables are obtained from the observations during fog. The output of a global non-hydrostatic NWP model is used in the diagnostic method to predict fog in winter months of 2018-2019. The study is divided into different sections. The next section describes the diagnostic method for fog forecast. Section 3 describes the global model. Section 4 describes the results of the study and summary with conclusions is given in section 5.

2. Diagnostic Method for Fog Forecast

The diagnostic method used in the present work is based on the combination of meteorological variables involved in fog formation such as temperature, humidity and wind speed. The study considers the following criteria to derive fog forecast:

Surface relative humidity over an appropriate threshold

Difference between surface temperature and surface dew point temperature .i.e. dew point depression under an appropriate threshold

Wind speed at 10 m between two appropriate thresholds.

The thresholds of these variables are obtained from the observations during fog during three years (2016-2019) in winter months at three stations Amritsar, Delhi and Lucknow situated in north India. The presence of fog is identified based on the observed values of visibility from METAR observations at all the three sites. Fog is considered when the observed visibility is reported less than 1000 m.

The analysis of visibility observations for the months of December, January and February during 2016-2019, suggests that fog observed for 1071, 1851 and 823 hours at Amritsar, Delhi and Lucknow respectively. The frequency of dense fog hours with observed values of visibility <200 m was highest over Amritsar and comparable over Delhi and Lucknow. The meteorological conditions during the fog hours were analyzed using the METAR observations of surface temperature (T), dew point depression (T-T_d), wind speed (WS) and specific humidity (SH). The values of relative humidity (RH) and specific humidity (SH) are obtained using the following equations.

$$RH = 100 - 5 \times (T - T_d) \tag{1}$$

$$SH = 6.1 \times 10^{\frac{(7.5 \times T_d)}{(237.3 + T_d)}} \tag{2}$$

During the fog hours, Amritsar observed high values of relative humidity close to 100% for maximum number of hours whereas the observed values of relative humidity lie in the range of 90%-100% for most of the hours over Delhi. Similarly, over Lucknow the observed values of relative humidity were 95%-100% for majority of hours. The dew point depression (difference between the temperature (T) and dew point temperature (T_d), T-T_d) was found zero at all the stations for majority of hours. The analysis of wind speed shows that weak surface winds of magnitude less than 2 m·s⁻¹ prevailed at all the stations during the fog hours. The mean (M) and standard deviation (STDEV) values of the variables, calculated using Equation (3) and Equation (4) respectively are given in Table 1.

$$M = \frac{\sum x}{n} = \bar{x} \tag{3}$$

$$STDEV = \frac{\sqrt{(x - \bar{x})^2}}{n} \tag{4}$$

where x denotes any of the variable such as RH, T-T_d, WS, T, SH and n is the total number of observations available at any station.

The mean values indicate the highest relative humidity, lowest dew-point depression, temperature and specific

humidity over Amritsar. The mean value explains the tendency of the data to assume certain values and the quantification of dispersion of data is given in terms of the value of standard deviation. The thresholds values of T-T_d, RH and WS required for fog formation are computed using the mean and standard deviation values of these variables at each station. The threshold of RH and minimum WS is obtained as mean minus standard deviation while the threshold of T-T_d and maximum WS as mean plus standard deviation and are given in Table 2. The threshold of relative humidity is highest over Amritsar and lowest over Delhi, whereas the threshold of dew point depression is lowest over Amritsar and highest over Delhi. However, in case of wind speed the minimum and maximum wind speed required for fog formation is the lowest and highest over Delhi.

Table 1. Mean, standard deviation for surface relative humidity (RH), dew point depression (T-T_d) and wind speed (WS) during fog hours at Amritsar, Delhi and Lucknow

Amritsar					
	RH (%)	T-T _d (°C)	WS (m·s ⁻¹)	T (°C)	SH (g/kg)
Mean	98.02	0.39	0.31	9.23	11.61
Standard Deviation	4.81	0.96	0.76	3.46	2.73
Delhi					
	RH (%)	T-T _d (°C)	WS (m·s ⁻¹)	T (°C)	SH (g/kg)
Mean	92.23	1.55	1.55	11.36	12.30
Standard Deviation	8.37	1.67	3.22	3.19	2.21
Lucknow					
	RH (%)	T-T _d (°C)	WS (m·s ⁻¹)	T (°C)	SH (g/kg)
Mean	95.55	0.89	0.51	10.47	12.56
Standard Deviation	5.43	1.09	0.83	8.35	2.86

Table 2. Thresholds for surface relative humidity, T-T_d and wind speed at Amritsar, Delhi and Lucknow

	Amritsar	Delhi	Lucknow
RH (%)	93.23%	83.86	90.12
T-T _d (°C)	1.35	3.22	1.97
WS10 (m·s ⁻¹)	0.44-1.07	0.21-2.88	0.32-1.33

Thus, fog will be observed over Amritsar, Delhi and Lucknow whenever the values of relative humidity, dew point depression and wind speed will be probably equal to their respective thresholds.

3. Model Details

The operational global Unified Model (UM) of NCM-RWF, (NCUM), used in the present study is developed at United Kingdom's Meteorological Office (UKMO). The model has a horizontal resolution of 17 km and 70 vertical levels with model top at 80 km. The dynamical core of the model uses semi-implicit, semi-Lagrangian formulation to solve the non-hydrostatic, fully compressible, deep atmospheric equations of motion^[42]. The primary atmospheric prognostic variables are three-dimensional (3-D) wind components, virtual dry potential temperature, Exner pressure and dry density, whilst the moist prognostic variables such as mass mixing ratio of water vapor, prognostic cloud fields and other atmospheric loadings are advected as free tracers. The Arakawa C-grid staggering^[43] is used for horizontal discretization of prognostic fields on to a regular latitude-longitude, whereas Charney-Philips staggering^[44] using terrain following hybrid height coordinated is used for vertical discretization. The 4D-Var data assimilation scheme is used to prepare initial conditions four times (00, 06, 12 and 18 UTC) a day^[45]. A deterministic ten-day forecast is generated daily based on 00 UTC initial conditions. The physical processes in the model are parameterized using different parameterization schemes. The radiation scheme of Edward and Slingo^[46] with nine bands in long wave and six bands in short wave region is used to parameterize the radiative processes. The atmospheric boundary layer is parameterized with turbulence closure scheme of Lock et al.^[47], which is further modified as described in Lock^[48] and Brown et al.^[49]. The Joint UK Land Environment Simulator (JULES) surface model^[50,51] is used to model the land surface and its interactions with atmosphere. Convection in the model is represented through a mass flux scheme based on Gregory and Rowntree^[52]. The prognostic cloud fraction and prognostic condensate (PC2) scheme is used for clouds and large-scale precipitation is represented using Wilson and Ballard^[53]. The details of terrain such as soil properties, land use, vegetation albedo and the distribution of natural and anthropogenic emissions at lower boundary are specified using ancillary files from different sources Walters et al.^[54].

4. Results & Discussion

The forecasted values of relative humidity, dew point depression and wind speed from NCUM are utilized in the diagnostic method to predict fog over the three stations. Thus, the performance of the model is first analyzed by comparing these meteorological variables obtained from model with the observations. Secondly, the thresholds obtained from the observations are applied to the output of model to forecast fog over a region. The output of the meteorological variables and the diagnostic method for fog forecast is verified during December 2018 through February 2019 over three stations Amritsar, Delhi and Lucknow.

4.1 Performance Analysis of NCUM

The forecast of temperature, dew point temperature, relative humidity and wind speed from NCUM are compared with observations at Amritsar, Delhi and Lucknow. The model output for the first 30 hours of the run is evaluated at each station for the fog hours during December 2018 to February 2019. The number of fog hours reported at Amritsar, Delhi and Lucknow are 134, 321 and 118, respectively. Fog at each station is reported between 18 UTC -23 UTC and 00 UTC- 06 UTC. Thus, the forecast of 18 hours to 30 hours based on 00 UTC initial conditions are compared with observations at each station.

The scatter diagram for observed and predicted surface temperature at three sites is shown Figure 1. The temperature over Amritsar (Figure 1 a) and Lucknow (Figure 1c) is over predicted by NCUM, whereas both under prediction and over prediction is observed over Delhi (Figure 1b).

Similarly, for dew point temperature the forecasted values are both over and under predicted over Amritsar (Figure 2a) and under predicted for majority of hours at Delhi (Figure 2b) and Lucknow (Figure 2c).

The forecast of relative humidity is highly under predicted at all the stations (Figure 3), whereas the forecast of wind speed is over predicted at all the stations (Figure 4).

The statistical scores such as bias, mean absolute error (MAE), root mean square error (RMSE) and correlation coefficient (R) are computed for each station and are given in Table 3. The scores indicate the highest correlation between the observed and forecasted values of temperature and dew point temperature. The values of RMSE are comparable for temperature, dew point temperature and wind speed whereas very high values are obtained for relative humidity at all the stations.

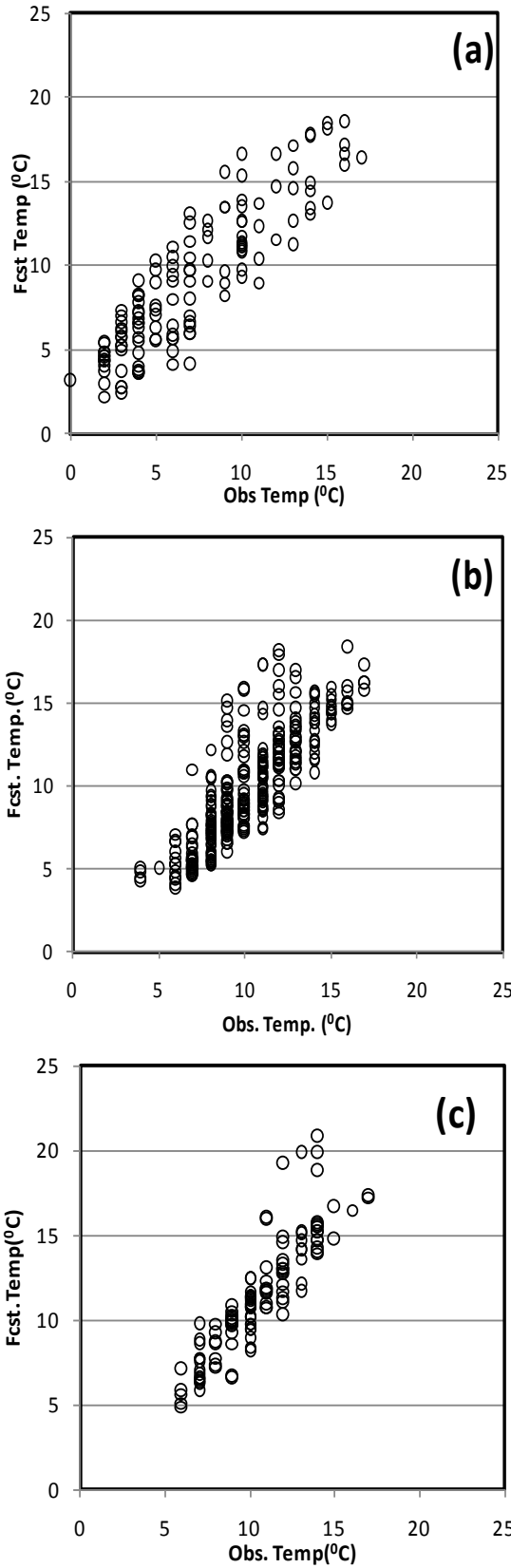


Figure 1. Scatter diagram of observed (Obs) (METAR) and forecasted (Fcst) (NCUM) temperature (Temp) at (a) Amritsar (b) Delhi and (c) Lucknow

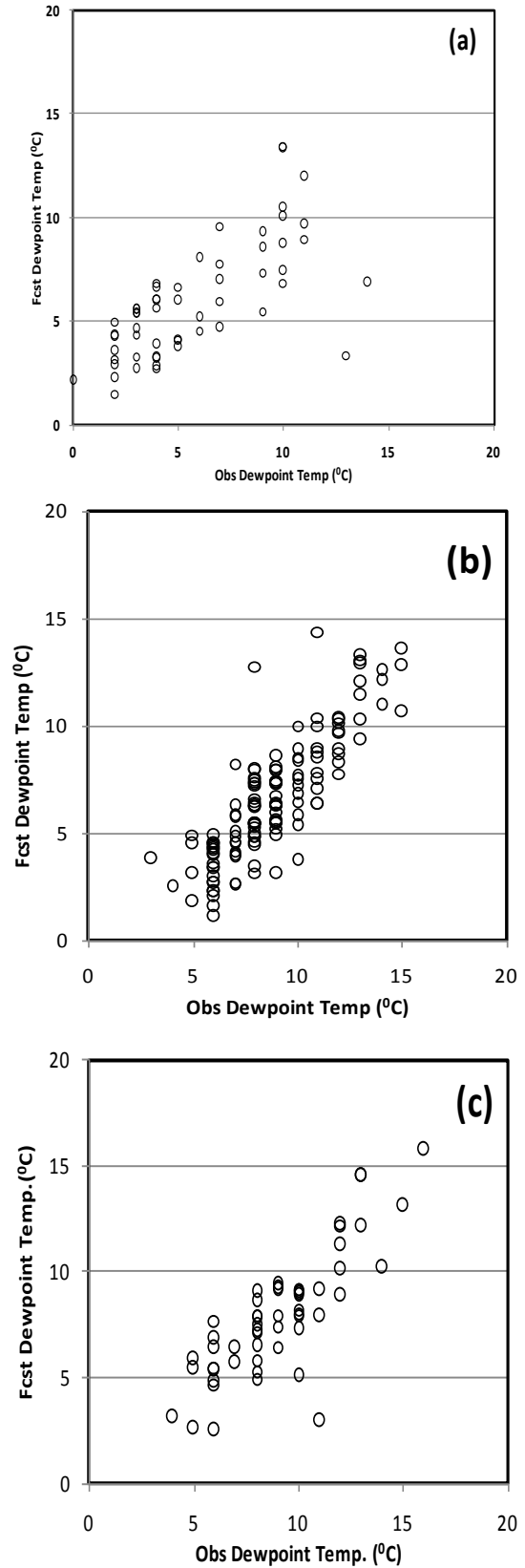


Figure 2. Scatter diagram of observed (Obs) (METAR) and forecasted (Fcst) (NCUM) dew point temperature at (a) Amritsar (b) Delhi and (c) Lucknow

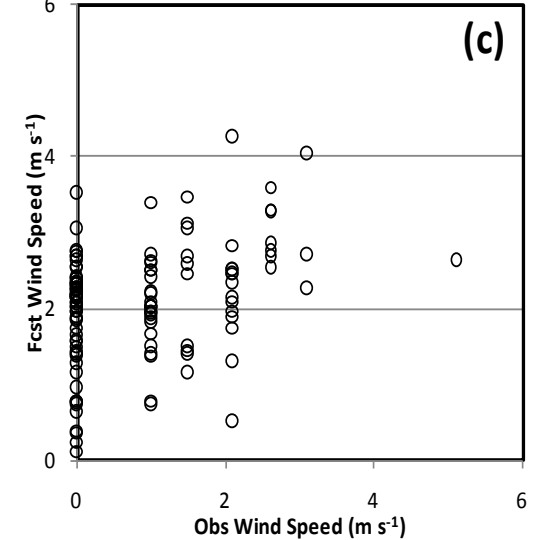
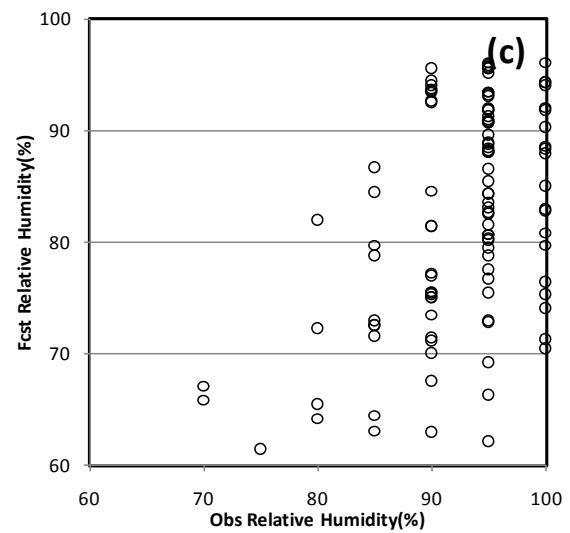
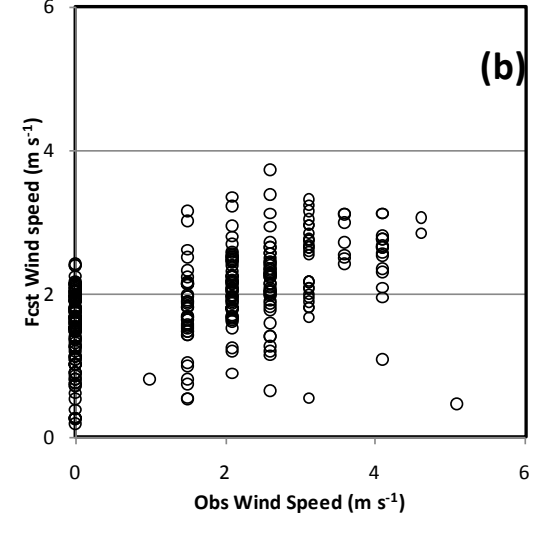
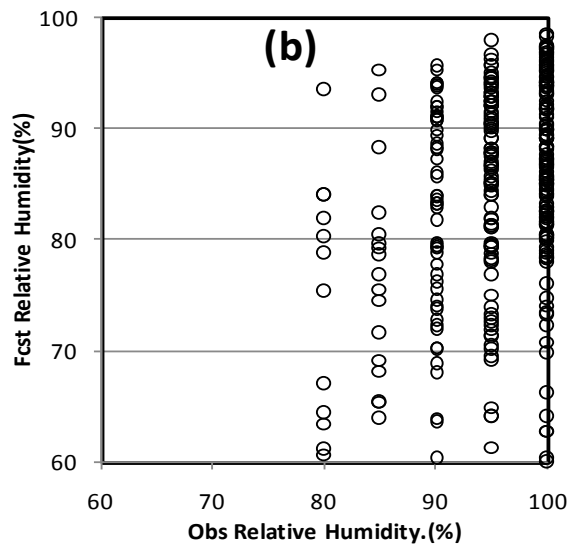
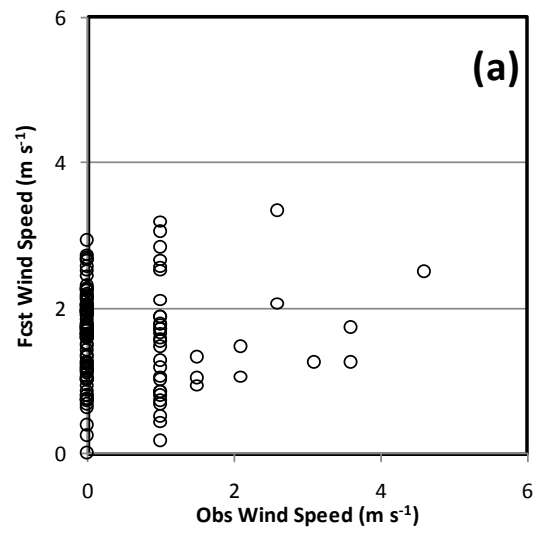
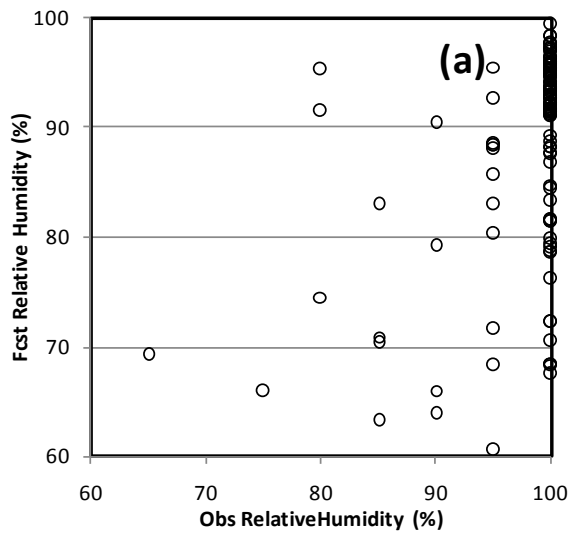


Figure 3. Scatter diagram of observed (Obs) (METAR) and forecasted (Fcst) (NCUM) relative humidity at (a) Amritsar (b) Delhi and (c) Lucknow

Figure 4. Scatter diagram of observed (Obs) (METAR) and forecasted (Fcst) (NCUM) wind speed at (a) Amritsar (b) Delhi and (c) Lucknow

Table 3. Statistical analysis of NCUM performance at three stations

Amritsar				
	Bias	RMSE	Correlation	MAE
Temperature	1.93	2.77	0.88	2.28
Dew-Point Temperature	0.16	2.41	0.71	1.80
Relative Humidity	-12.04	16.60	0.53	12.51
Wind Speed	1.14	1.62	0.14	1.43
Delhi				
	Bias	RMSE	Correlation	MAE
Temperature	-0.34	1.93	0.83	1.49
Dew-Point Temperature	-2.23	2.74	0.84	2.40
Relative Humidity	-11.90	15.62	0.49	12.50
Wind Speed	0.38	1.22	0.54	0.96
Lucknow				
	Bias	RMSE	Correlation	MAE
Temperature	0.83	1.86	0.88	1.29
Dew-Point Temperature	-1.14	2.05	0.82	1.52
Relative Humidity	-11.50	14.97	0.54	12.13
Wind Speed	1.22	1.60	0.36	1.35

A positive bias for temperature with higher values over Amritsar than Lucknow indicates an over-prediction which agrees with scatter plot (Figure 1a and 1c). Similarly, the lowest negative bias in temperature values over Delhi indicates the least under prediction. For dew point temperature the lowest bias is obtained for Amritsar. A positive bias is obtained for wind speed with comparable magnitude at all the stations. The values of MAE for temperature, dew point temperature and wind speed are comparable at all the stations and lowest MAE is obtained for wind speed over Delhi.

4.2 Performance of the Diagnostic Method in Predicting Fog

The diagnostic method is based on the threshold of relative humidity, dew point depression and wind speed obtained from observations at three selected stations. These thresholds are applied to the observed and forecasted values of relative humidity, dew point depression and wind speed over Amritsar, Delhi and Lucknow for the fog hours during 2018-2019.

The diagnostic method of fog forecast is evaluated by computing the statistical scores such as accuracy, probability of detection (POD), false alarm ratio (FAR), success ratio (SR) and threat score (TS) (WWRP)^[55]. These indices are computed based on the frequency of positive and negative occurrences such as:

Hits are the events for which both the forecasted and observed values of variables are within the thresholds defined over any given station.

Correct Negatives (CN) are the events when both forecasted and observed values of variables are greater than or lower than the thresholds defined over the station.

False Alarms are those events when forecasted values are within the thresholds but not the observed values and **Misses** are the events when observed values are within the thresholds but not the forecasted values.

A perfect system should produce only hits and correct negatives (CN) and a positive event in the present work is represented by the correct detection/forecast of fog presence.

The forecast of fog over Amritsar, Delhi and Lucknow is verified using the Yes/No forecast and the statistical scores. For 134 hours of fog observed at Amritsar, the diagnostic method gave Hits for 55 hours, Misses for 59 hours, False Alarm for 01 hour and Correct Negative for 19 hours. Similarly, over Delhi the fog was observed for 321 hours and was predicted for 175 hours (Hits), not predicted for 119 hours (Misses), falsely predicted for 07 hour (false Alarm) and for 20 hours the fog was neither observed and nor predicted. In case of Lucknow, there were 118 hours of fog out of which the number of Hits were obtained for 08 hours, Misses for 63 hours, False Alarm for 01 hour and Correct Negatives for 46 hours.

The statistical scores are computed using the number of Hits, Misses, False Alarms and Correct Negatives over Amritsar, Delhi and Lucknow and are shown in Figure 5. The highest POD (0.60), threat score (0.58) and accuracy (0.61) with FAR of 0.04 is obtained over Delhi. The performance of diagnostic method in predicting fog over Amritsar is comparable to Delhi with POD of 0.48, threat score of 0.48, accuracy of 0.55 and FAR of 0.02. The scores over Lucknow indicate that diagnostic method failed to predict fog for majority of hours.

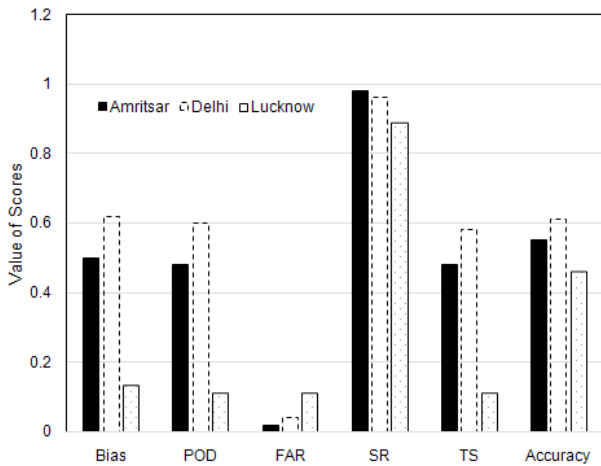


Figure 5. Statistical Scores at Amritsar, Delhi and Lucknow for performance of the diagnostic method

5. Conclusions

In this study, a diagnostic method is used for forecasting fog over three stations Amritsar, Delhi and Lucknow situated in the northern plains of India. The diagnostic method is based on the thresholds of relative humidity, dew point depression and wind speed for the formation of fog. The thresholds are computed at each of the station using the observations of winter months (December-February) for three years 2016-2019 during fog. The output of NCUM is used to predict fog with diagnostic method over Amritsar, Delhi and Lucknow. The study includes the performance analysis of NCUM in predicting surface temperature, dew point temperature, relative humidity and wind speed at three stations. The verification of diagnostic method is also carried out using the Yes/No forecast for the winter months of 2018-2019. The main findings of the study are summarized as follows:

The threshold of relative humidity for the formation of fog is found lowest over Delhi (83.86%) and highest over Amritsar (93.23%). The threshold of dew point depression is highest over Delhi and lowest over Amritsar. For wind speed the minimum threshold is lowest and maximum

threshold is highest over Delhi.

The performance of NCUM in predicting temperature, dew point temperature and wind speed is found comparable to observations at all the stations, however the relative humidity is over-predicted by NCUM at all the stations.

Considering the three sites, the diagnostic method is able to predict fog in the 18-30 hour forecast with an overall accuracy of 0.54 and a probability of false detection equal to 0.11. The performance of the diagnostic method is found best over Delhi and comparable to Amritsar, whereas the fog is poorly predicted over Lucknow.

The averaged bias of 0.42 together with low value of probability of false detection indicates that the method produces a consistent number of missed fog events.

The average of success ratio is 0.94, which means that 94% of the fog events forecasted by the model have been actually observed.

Acknowledgements

The authors acknowledge the National Centre for Medium Range Weather Forecasting (NCMRWF), Noida, India for the global NCUM products. There is no funding source and no conflict of interest.

Conflict of Interest

There is no conflict of interest.

References

- [1] Gultepe, I., Tardif, R., Michaelides, S.C., et al., 2007. Fog research: A review of past achievements and future perspectives. *Pure and Applied Geophysics*. 164(6), 1121-1159.
- [2] Jenamani, R.K., Tyagi, A., 2011. Monitoring fog at IGI Airport and analysis of its runway-wise spatio-temporal variations using Meso-RVR network. *Current Science*. 100, 491-501.
- [3] Bergot, T., 2013. Small-scale structure of radiation fog: a large eddy simulation study. *Quarterly Journal of Royal Meteorological Society*. 139, 1099-1112.
- [4] Haeffelin, M., Laffineur, Q., Bravo-Aranda, J.A., et al., 2016. Radiation fog formation alerts using attenuated backscatter power from automatic lidars and ceilometers. *Atmospheric Measurement Techniques*. 9(11), 5347-5365. DOI: <https://doi.org/10.5194/amt-9-5347-2016>
- [5] Singh, A., George, J.P., Iyengar, G.R., 2018. Prediction of fog/visibility over India using NWP Model. *Journal of Earth System Science*. 127(2), 26. DOI: <https://doi.org/10.1007/s12040-018-092-2>
- [6] Croft, P.J., 2003. Fog. *Encyclopedia of atmospheric*

- sciences. J. R. Holton, J. A. Pyle, J. A. Curry (Eds.), Academic Press. pp. 777-792.
- [7] Forthun, G., Johnson, M., Schmitz, W., et al., 2006. Trends in fog frequency and duration in the southeast United States. *Physical Geography*. 27, 206-222. DOI: <https://doi.org/10.2747/0272-3646.27.3.206>
- [8] Gultepe, I., Tardif, R., Michaelides, S.C., et al., 2007. Fog research: A review of past achievements and future perspectives. *Pure and Applied Geophysics*. 164(6), 1121-1159.
- [9] Gultepe, I., Pearson, G., Milbrandt, J.A., et al, 2009. The fog remote sensing and modeling field project. *Bulletin of American Meteorological Society*. 90, 341-359. DOI: <https://doi.org/10.1175/2008BAMS2354.1>
- [10] Kulkarni, R.G., et al., 2019. Loss to aviation economy due to winter fog in New Delhi during the winter of 2011–2016. *Atmosphere*. 10, 198-210.
- [11] Tardif, R., Rasmussen, R.M., 2007. Event-based climatology and typology of fog in the New York City region. *Journal of Applied Meteorology and Climatology*. 46, 1141-1168.
- [12] Ghude, S.D., Bhat, G.S., Prabhakaran, T., et al., 2017. Winter fog experiment over the Indo-Gangetic plains of India. *Current Science*. 112, 767-784. DOI: <https://doi.org/10.18520/cs/v112/i04/767-784>
- [13] Izett, J.G., et al., 2019. Dutch fog: On the observed spatio-temporal variability of fog in the Netherlands. *Quarterly Journal of Royal Meteorological Society*. 145, 2817-2834.
- [14] Guerreiro, P.M.P., et al., 2020. An Analysis of Fog in the Mainland Portuguese International Airports. *Atmosphere*. 11, 1239-1260.
- [15] Brown, R., Roach, W.T., 1976. The physics of radiation fog II-a numerical study. *Quarterly Journal of Royal Meteorological Society*. 102, 351-354.
- [16] Holtslag, A.A.M., De Bruijin, E.I.F., Pan, H.L., 1990. A high resolution air mass transformation model for short-range weather forecasting. *Monthly Weather Review*. 118, 1561-1575.
- [17] Bergot, T., Guedalia, D., 1994. Numerical forecasting of radiation fog. Part I. Numerical model and sensitivity tests. *Monthly Weather Review*. 122, 1218-1230.
- [18] Fisak, J., Rezacova, D., Mattanen, J., 2006. Calculated and measured values of liquid water content in clean and polluted environments. *Studia Geophysica et Geodaetica*. 50, 121-130.
- [19] Bergot, T., Terradellas, E., Cuxart, J., et al., 2007. Intercomparison of single-column numerical models for the prediction of radiation fog. *Journal of Applied Meteorology and Climatology*. 46, 504-521.
- [20] Gultepe, I., Pagowski, M., Reid, J., 2007. A satellite-based fog detection scheme using screen air temperature. *Weather and Forecasting*. 22, 444-456. DOI: <https://doi.org/10.1175/WAF1011.1>
- [21] Haeffelin, M., Bergot, T., Elias, T., et al., 2009. Paris fog: Shedding new light on fog physical processes. *Bulletin of the American Meteorological Society*. 91(6), 767-783.
- [22] Liu, D.Y., Yang, J., Niu, Sh.J., et al., 2011. On the evolution and structure of a radiation fog event in Nanjing. *Advances in Atmospheric Sciences*. 28(1), 223-237.
- [23] Sun, K., 2015. WRF-chem simulation of a severe haze episode in the Yangtze River Delta, China. *Aerosol and Air Quality Research*. DOI: <https://doi.org/10.4209/aaqr.2015.04.0248>
- [24] Lin, C.Y., Zhang, Zh.F., Pu, Zh.X., 2017. Numerical simulations of an advection fog event over Shanghai Pudong International Airport with the WRF model. *Journal of Meteorological Research*. 31, 874-889.
- [25] Boutle, I., Price, J., Kudzotsa, I., et al., 2018. Aerosol–fog interaction and the transition to well-mixed radiation fog. *Atmospheric Chemistry and Physics*. 18(11), 7827-7840. DOI: <https://doi.org/10.5194/acp-18-7827-2018>
- [26] Pithani, P., Ghude, S.D., Chennu, V.N., et al., 2018. WRF model Prediction of a dense fog event occurred during Winter Fog Experiment (WIFEX). *Pure and Applied Geophysics*. DOI: <https://doi.org/10.1007/s00024-018-2053-0>
- [27] Price, J.D., Lane, S., Boutle, I.A., et al., 2018. LAN-FEX: A field and modeling study to improve our understanding and forecasting of radiation fog. *Bulletin of the American Meteorological Society*. 99(10), 2061-2077. DOI: <https://doi.org/10.1175/BAMS-D-16-0299.1>
- [28] Pasricha, P.K., et al., 2003. Role of water vapour green house effect in the forecasting of fog occurrence. *Boundary Layer Meteorology*. 107, 469-482. DOI: <https://doi.org/10.1023/A:1022128800130>
- [29] Dimri, A.P., Barros, N., Ridley, P.A., et al., 2015. Western disturbances: A review. *Reviews of Geophysics*. 53, 225-246. DOI: <https://doi.org/10.1002/014RG000460>
- [30] Choudhury, S., Rajpala, H., Sarafa, A.A., et al., 2007. Mapping and forecasting of north Indian winter fog: an application of spatial technologies. *International Journal of Remote Sensing*. 28, 3649-3663.
- [31] Chakraborty, A., Gupta, T., Tripathi, S.N., 2016. Combined effects of organic aerosol loading and fog

- processing on organic aerosols oxidation, composition and evolution. *Science of Total Environment*. 573, 690-698.
- [32] Jenamani, R.K., 2007. Alarming rise in fog and pollution causing a fall in maximum temperature over Delhi. *Current Science*. 93, 314-322.
- [33] Syed, F.S., Körnich, H., Tjernstrom, M., 2012. On the fog variability over South Asia. *Climate Dynamics*. 39, 2993-3005.
DOI: <https://doi.org/10.1007/s00382-012-1414-0>
- [34] Kulkarni, R.G., et al., 2019. Loss to aviation economy due to winter fog in New Delhi during the winter of 2011–2016. *Atmosphere*. 10, 198-210.
- [35] Stull, R.B., 1988. *An Introduction to Boundary layer Meteorology*, Kluwer Academic Publishers. pp. 666.
- [36] Kunkel, B.A., 1984. Parameterization of droplet terminal velocity and extinction coefficient in fog models. *Journal of Climate and Applied Meteorology*. 23, 34-41.
- [37] Zhou, B., Du, J., 2010. Fog prediction from a multimodel mesoscale ensemble prediction system. *Weather and Forecasting*. 25, 303-322.
- [38] Zhou, B.B., Du, J., Gultepe, I., et al., 2011. Forecast of Low Visibility and Fog From NCEP– Current Status and Efforts. *Pure and Applied Geophysics*. 169, 895-909.
- [39] Aditi, et al., 2015. Verification of Visibility Forecast from NWP model with Satellite and Surface Observations. *Mausam*. 66, 603-616.
- [40] Zhou, B., Ferrier, B.S., 2008. Asymptotic analysis of equilibrium in radiation fog. *Journal of Applied Meteorology and Climatology*. 47, 1704-1722.
- [41] Payra, S., Mohan, M., 2014. Multirule Based Diagnostic Approach for the Fog Predictions Using WRF Modelling Tool. *Advances in Meteorology*. pp. 1-11.
DOI: <https://doi.org/10.1155/2014/456065>
- [42] Wood, N., Staniforth, A., White, A., et al., 2014. An inherently mass-conserving semi-implicit semi-Lagrangian discretization of the deep-atmosphere global nonhydrostatic equations. *Quarterly Journal of Royal Meteorological Society*. 140, 1505-1520.
DOI: <https://doi.org/10.1002/qj.2235>, 2014
- [43] Arakawa, A., Lamb, V.R., 1977. Computational design of the basic dynamic processes of the UCLA general circulation model. *Methods in Computational Physics*. *Advances in Research and Applications*. 17, 173-265.
- [44] Charney, J.G., Phillips, N.A., 1953. Numerical integration of the quasi-geostrophic equations for barotropic and simple baroclinic flows. *Journal of Meteorology*. 10, 71-99.
- [45] George, J.P., et al., 2016. NCUM data assimilation system. NMRF/TR/01/2016.
- [46] Edwards, J.M., Slingo, A., 1996. Studies with a flexible new radiation code. I: Choosing a configuration for a largescale model. *Quarterly Journal of Royal Meteorological Society*. 122, 689-719.
- [47] Lock, A.P., Brown, A.R., Bush, M.R., et al., 2000. A new boundary layer mixing scheme. Part I: Scheme description and single-column model tests. *Monthly Weather Review*. 128, 3187-3199.
- [48] Lock, A.P., 2001. The numerical representation of entrainment in parametrizations of boundary layer turbulent mixing, *Monthly. Weather Review*. 129, 1148-1163.
- [49] Brown, A.R., et al., 2008. Upgrades to the boundary-layer scheme in the Met Office numerical weather prediction model. *Boundary Layer Meteorology*. 128, 117-132.
DOI: <https://doi.org/10.1007/s10546-008-9275-0>
- [50] Best, M.J., Pryor, M., Clark, D.B., et al., 2011. The Joint UK Land Environment Simulator (JULES), model description –Part 1: Energy and water fluxes. *Geoscientific Model Development*. 4, 677-699.
- [51] Clark, D.B., Mercado, L.M., Sitch, S., et al., 2011. The Joint UK Land Environment Simulator (JULES), model description – Part 2: Carbon fluxes and vegetation dynamics. *Geoscientific Model Development*. 4, 701-722.
- [52] Gregory, D., Rowntree, P.R., 1990. A massflux convection scheme with representation of cloud ensemble characteristics and stability dependent closure. *Monthly Weather Review*. 118, 1483-1506.
- [53] Wilson, D.R., Ballard, S.P., 1999. A microphysically based precipitation scheme for the UK Meteorological Office Unified Model. *Quarterly Journal of Royal, Meteorological, Society*. 125, 1607-1636.
DOI: <https://doi.org/10.1002/qj.49712555707>
- [54] Walters, D., Brooks, M., Boutle, I., et al., 2017. The Met Office Unified Model Global Atmosphere 6.0/6.1 and JULES Global Land 6.0/6.1 configurations. *Geoscientific Model Development*. 10, 1487-1520.
DOI: <https://doi.org/10.5194/gmd-10-1487-2017>
- [55] WWRP/WGNE Joint Working Group on Forecast Verification Research. Available online: <https://www.cawcr.gov.au/projects/verification/> (Accessed on 13 December 2019).